Histone methyltransferase DOT1L is essential for self-renewal of germline stem cells

Huijuan Lin, Keren Cheng, Hiroshi Kubota, Yemin Lan, Simone S. Riedel, Kazue Kakiuchi, Kotaro Sasaki, Kathrin M. Bernt, Marisa S. Bartolomei, Mengcheng Luo & P. Jeremy Wang

SUPPLEMENTAL INFORMATION

- Supplemental Materials and Methods
- Supplemental References
- Four supplemental table legends
- Seven supplemental figures with legends

Supplemental Materials and Methods

Generation of anti-DOT1L antibody

The mouse *Dot1l* cDNA fragment encoding aa 551-847 was cloned into the pQE-30 vector (QIAGEN) to express a 6×His-DOT1L recombinant protein. The fusion protein was expressed in M15 bacteria, purified with Ni-NTA resin, and eluted in 8 M urea. Two rabbits were immunized at Cocalico Biologicals, resulting in antiserum UP2565. Affinity purified anti-DOT1L antibody was used for immunofluorescence (1:50).

Sperm count and mating test

For sperm count, one cauda epididymis from each mouse was harvested and placed in a tissue dish with 1×DPBS. The cauda was minced into small pieces with scissors, fixed in paraformaldehyde, and counted on the Hausser Bright-Line hematocytometer. For each mating test, one 8-week-old *Dot1l*$^{fl/-}$ *Ddx4*-Cre or control male was mated with two 8-week-old wild-type females for 2 months. The litter number and size during this period were recorded.

Histological, immunofluorescence, TUNEL and BrdU analyses

For histological analysis, testes were fixed in Bouin's solution, subsequentially dehydrated with gradient alcohol, embedded with paraffin, and sectioned. Sections were deparaffinized in xylene, rehydrated with gradient alcohol, and stained with hematoxylin and eosin. Sections were imaged on a Leica DM5500B microscope by DFC450 digital color camera (Leica Microsystems). Two hours before harvest of the testes, a single dose of BrdU (Sigma, B5002) was injected intraperitoneally into the *Dot1l*$^{fl/fl}$ *Ddx4*-Cre^{ERT2} and *Dot1l*$^{fl/+}$ *Ddx4*-Cre^{ERT2} males (50 mg/kg of body weight) after tamoxifen treatment described above. For immunofluorescence including TUNEL and BrdU analyses, testes were fixed in 4% paraformaldehyde (in PBS) overnight at 4°C, dehydrated in 30% sucrose (in PBS) overnight, embedded in optimal cutting temperature compound (#6502, Thermo Scientific), and sectioned on a cryostat. Alternatively, fixed testes were dehydrated with gradient alcohol, embedded in paraffin, and sectioned on a microtome. Paraffin-embedded slides were deparaffinized in xylene, rehydrated with gradient alcohol. Heat-induced epitope retrieval was performed for the rehydrated slides by incubation in the epitope retrieval buffer (1 mM EDTA buffer, 0.05% Tween-20, pH 8.0) at 95°C for 20 minutes, excluding TUNEL assays. Epitope retrieval for TUNEL assays was performed with incubation

with proteinase K (10 μg/ml) at room temperature for 10 minutes. Subsequently, slides were incubated with 0.5% Triton X-100 in 1×PBS at room temperature for 10 minutes. For in vitro cultured cells, cells were fixed in 2% paraformaldehyde (in PBS) on slides (#12-550-15, Fisher Scientific) and incubated in a humidified chamber at 4°C for 3 hours or overnight. After fixation, the slides were air-dried and washed in 0.4% Photo-Flo 200 solution (Kodak, 1464510) three times.

The slides were blocked with 10% goat serum in PBST at 37°C for 1 hour followed by antibody incubation at 37°C overnight. The primary antibodies used for immunofluorescence were as follows: SALL4 (1:200, ab29112, Abcam), GCNA1 (1:100, 10D9G11-s, DSHB), hLIN28A (1:100, AF3757, R&D system), H3K79me2 (1:100, ab3594, Abcam), BrdU (1:100, ab6326, Abcam), and SP10 (1:100, from Prabhakara Reddi, University of Illinois) (Osuru et al. 2014). Secondary antibodies were FITC- or Texas red-conjugated. TUNEL assays were performed with the TUNEL kit, namely TUNEL Enzyme (#11767305001, Roche) and TUNEL Label (#11767291910, Roche) at a ratio of 1:10. Mounting medium with DAPI (H-1200, VECTASHIELD) was added for nuclear DNA counterstaining and fluorochrome preservation. Fluorescence images were captured with an ORCA Flash4.0 digital monochrome camera (Hamamatsu Photonics) on a Leica DM5500B microscope (Leica Microsystems).

Western blotting analysis

Total protein extract from testis or cultured cells was prepared by homogenization in 5 volumes of protein extraction buffer (62.5 mM Tris-HCl pH 6.8, 3% SDS, 10% glycerol, 5% 2-mercaptoethanol), and boiled at 95°C for 15 minutes followed by centrifugation at 12000 rpm for 5 minutes. Samples were run in an SDS-PAGE gel, and then transferred to the PVDF membrane. The membrane blot was blocked in 5% non-fat milk (in PBST) at room temperature for 1 hour. The primary antibodies used for western blot were as follows: GCNA1 (1:1000, 10D9G11-s, DSHB), hLIN28A (1:1000, AF3757, R&D system), DOT1L (1:1000, ab64077, Abcam), H3K79me2 (1:1000, ab3594, Abcam), ACTB (1:5000, A5441, Sigma), and histone H3 (1:2000, 9715, Cell Signaling Technology). Secondary antibodies were HRP-conjugated. ECL western blotting substrate (32106, Thermo Fisher Scientific) was used for development.

Derivation of *Dot1l*$^{+/-}$ and *Dot1l*$^{-/-}$ spermatogonial stem cell lines

Dot1l$^{fl/fl}$ *Ddx4*-Cre^{ERT2} mice on a mixed genetic background were crossed with DBA/2J (Stock number 000671, Jackson Laboratory) mice to obtain *Dot1l*$^{fl/+}$ *Ddx4*-Cre^{ERT} and *Dot1l*$^{fl/fl}$ *Ddx4*-Cre^{ERT2} mice with a 50% DBA/2J background. SSCs were derived from *Dot1l*$^{fl/+}$ *Ddx4*-Cre^{ERT} and *Dot1l*$^{fl/fl}$ *Ddx4*-Cre^{ERT2} pups respectively. SSCs were cultured and passaged in the presence of 0.8 μM 4-hydroxytamoxifen (H6278, Sigma) for 42 days. SSC colonies were picked, expanded, and genotyped (Supplemental Fig. S6A). The *Dot1l*$^{+/-}$ *Ddx4*-Cre^{ERT2} SSC line was derived from *Dot1l*$^{fl/+}$ *Ddx4*-Cre^{ERT2} SSCs and the *Dot1l*$^{-/-}$ *Ddx4*-Cre^{ERT2} SSC line was derived from *Dot1l*$^{fl/fl}$ *Ddx4*-Cre^{ERT2} SSCs (Supplemental Fig. S6A).

Supplemental References

Boulet AM, Capecchi MR. 1996. Targeted disruption of hoxc-4 causes esophageal defects and vertebral transformations. *Dev Biol* **177**: 232-249.

Garcia-Gasca A, Spyropoulos DD. 2000. Differential mammary morphogenesis along the anteroposterior axis in Hoxc6 gene targeted mice. *Dev Dyn* **219**: 261-276.

Hostikka SL, Gong J, Carpenter EM. 2009. Axial and appendicular skeletal transformations, ligament alterations, and motor neuron loss in Hoxc10 mutants. *Int J Biol Sci* **5**: 397-410.

Hwang J, Mehrani T, Millar SE, Morasso MI. 2008. Dlx3 is a crucial regulator of hair follicle differentiation and cycling. *Development* **135**: 3149-3159.

Le Mouellic H, Lallemand Y, Brulet P. 1992. Homeosis in the mouse induced by a null mutation in the Hox-3.1 gene. *Cell* **69**: 251-264.

Morasso MI, Grinberg A, Robinson G, Sargent TD, Mahon KA. 1999. Placental failure in mice lacking the homeobox gene Dlx3. *Proc Natl Acad Sci U S A* **96**: 162-167.

Osuru HP, Monroe JE, Chebolu AP, Akamune J, Pramoonjago P, Ranpura SA, Reddi PP. 2014. The acrosomal protein SP-10 (Acrv1) is an ideal marker for staging of the cycle of seminiferous epithelium in the mouse. *Mol Reprod Dev* **81**: 896-907.

Saegusa H, Takahashi N, Noguchi S, Suemori H. 1996. Targeted disruption in the mouse Hoxc-4 locus results in axial skeleton homeosis and malformation of the xiphoid process. *Dev Biol* **174**: 55-64.

Suemori H, Takahashi N, Noguchi S. 1995. Hoxc-9 mutant mice show anterior transformation of the vertebrae and malformation of the sternum and ribs. *Mech Dev* **51**: 265-273.

Wellik DM, Capecchi MR. 2003. Hox10 and Hox11 genes are required to globally pattern the mammalian skeleton. *Science* **301**: 363-367.

Wellik DM, Hawkes PJ, Capecchi MR. 2002. Hox11 paralogous genes are essential for metanephric kidney induction. *Genes Dev* **16**: 1423-1432.

Supplemental Table Legends

Supplemental Table S1. RNA-seq analysis of SSCs treated with or without EPZ5676.

Supplemental Table S2. H3K79me2 ChIP peaks and classes of genes associated with peaks.

Supplemental Table S3. Phenotypes of *Homeobox* gene knockout mice.

Supplemental Table S4. qRT-PCR primer sequences.

Supplementary Figures

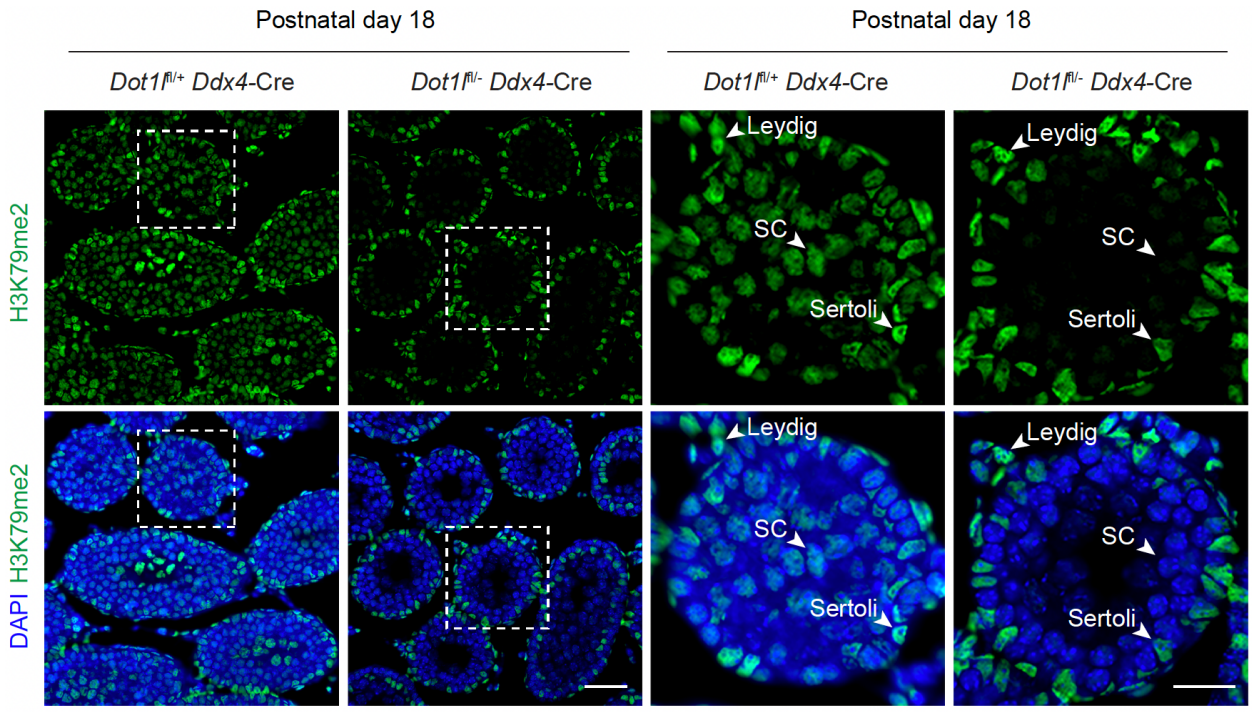

Supplemental Figure S1. Germ cell-specific loss of H3K79me2 in *Dot1l*^{cKO} (*Dot1l*$^{fl/-}$ *Ddx4*-Cre) testes at postnatal day 18 (P18). Left panels: immunofluorescence of H3K79me2 in control (*Dot1l*$^{fl/+}$ *Ddx4*-Cre) and *Dot1l*^{cKO} testes at P18 at a low magnification. Right panels: enlarged view of boxed tubules. DNA is stained with DAPI. Spermatocytes (SC), Sertoli cells and Leydig cells are labeled. Scale bars, 50 μm.

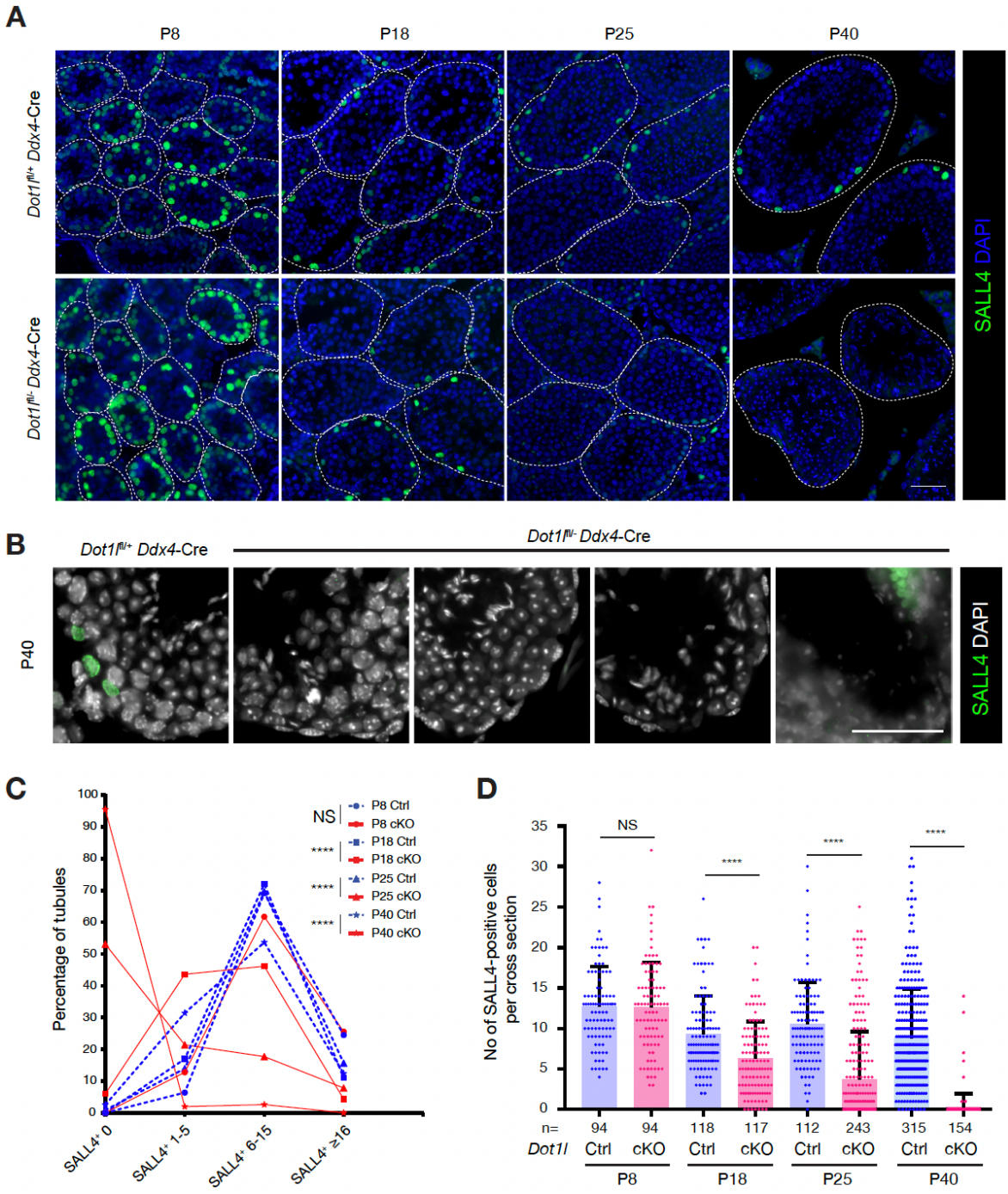

Supplemental Figure S2. Age-dependent progressive loss of SALL4^{+} spermatogonia in *Dot1l*^{cKO} (*Dot1l*$^{fl/-}$ *Ddx4*-Cre) testes. (A) Immunofluorescence of SALL4 in control (*Dot1l*$^{fl/+}$ *Ddx4*-Cre) and *Dot1l*^{cKO} testes at P8, P18, P25, and P40. Scale bar, 50 µm. (B) Immunofluorescence of SALL4 in control and *Dot1l*^{cKO} testes at P40. Scale bar, 50 µm. (C) Quantification of tubules with different numbers of SALL4^{+} spermatogonia in control and *Dot1l*^{cKO} testes at P8, P18, P25, and P40. (D) The average number of SALL4^{+} cells per cross section (excluding tubules with no SALL4^{+} spermatogonia). NS, not significant; ****, p<0.0001. P8 and P18 (C, D), unpaired Student's t-test; P25 and P40 (C, D), Mann Whitney U test.

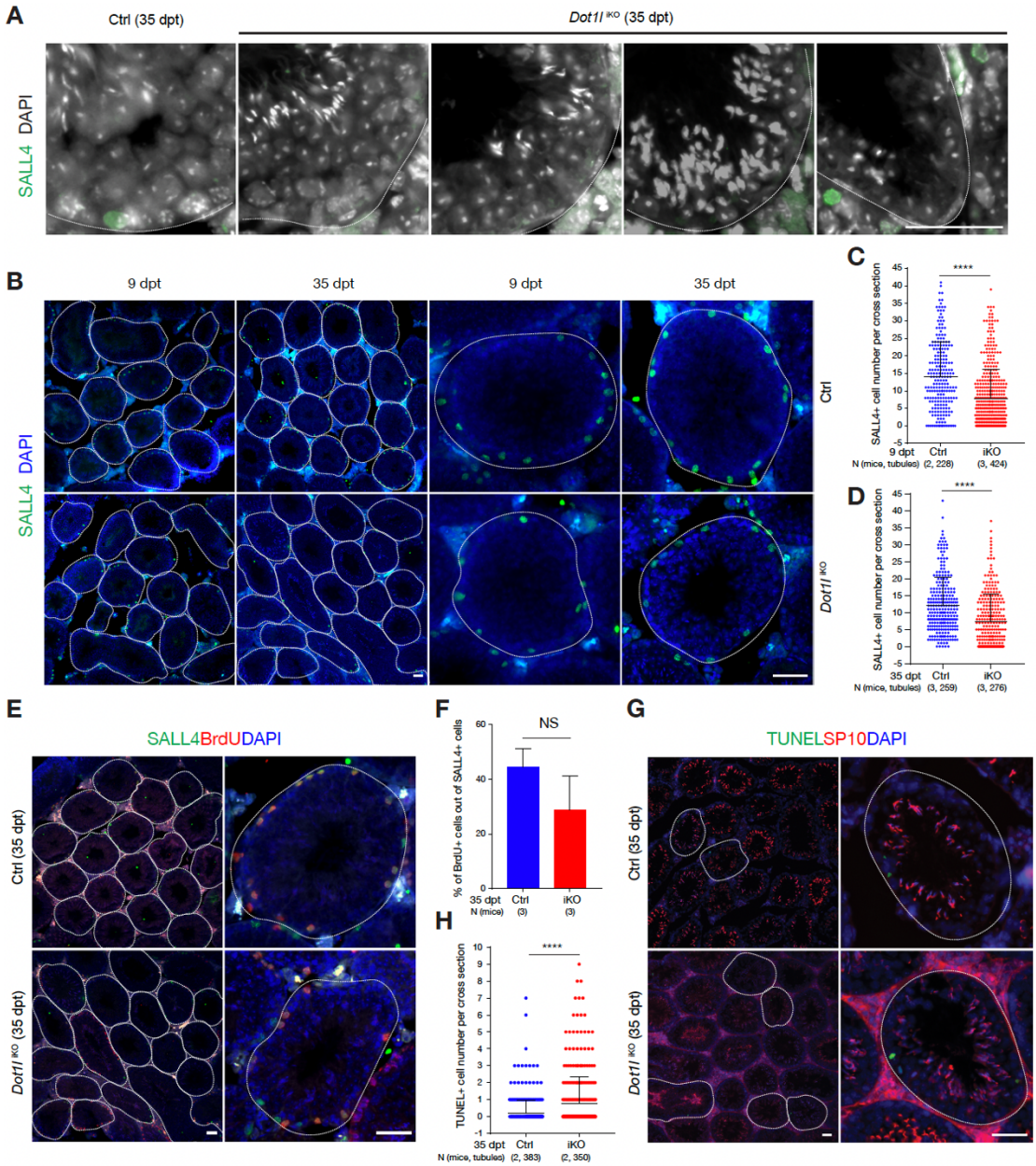

Supplemental Figure S3. SALL4 immunofluorescence, BrdU incorporation, and TUNEL analyses in *Dot1l*^{iKO} (*Dot1l*$^{fl/fl}$ *Ddx4*-Cre^{ERT2}) testes at 35 dpt. (A) Immunofluorescence of SALL4 in control and *Dot1l*^{iKO} testes at 35 dpt. Tubules with progressive germ cell depletion in *Dot1l*^{iKO} testes are shown. Scale bar, 50 µm. (B) Immunofluorescence of SALL4 in control and *Dot1l*^{iKO} testes at 9 dpt and 35 dpt. Representative images at two magnifications are shown. Scale bar, 50 µm. (C, D) Quantification of SALL4^{+} spermatogonia in control and *Dot1l*^{iKO} testes at 9 dpt (C) and 35 dpt (D). (E) Immunofluorescence of SALL4 and BrdU in control and *Dot1l*^{iKO} testes at 35 dpt. (F) Quantification of BrdU-positive cells in SALL4^{+} spermatogonia. (G) TUNEL analysis in control and *Dot1l*^{iKO} testes at 35 dpt. SP10 is an acrosomal marker (Osuru et al. 2014). Scale bar, 50 µm. (H) Quantification of TUNEL-positive cells per tubule cross section. NS, not significant; ****, $p<0.0001$, unpaired Student's *t*-test (C, D, F) or Mann Whitney *U* test (H).

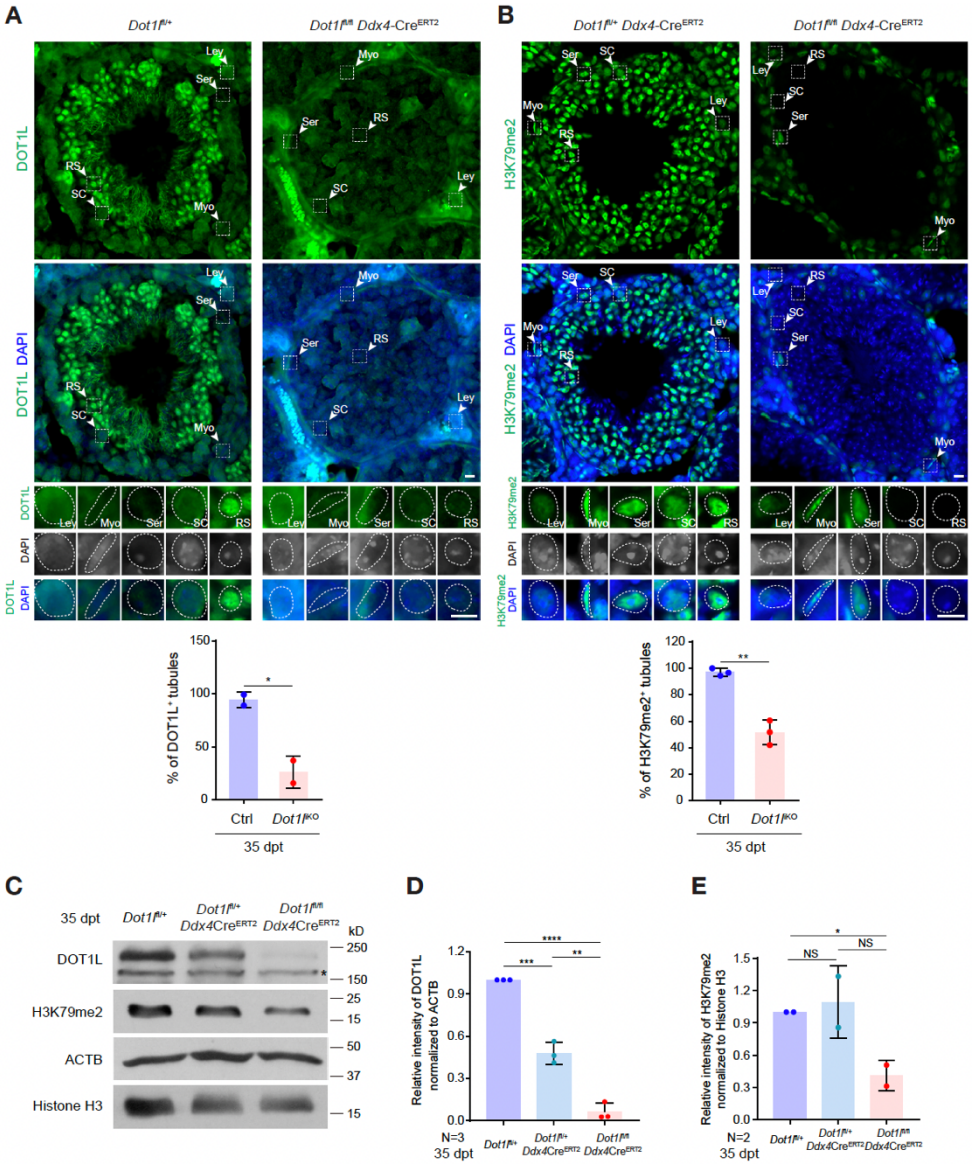

Supplemental Figure S4. Depletion of DOT1L and H3K79me2 in adult *Dot1l*^{iKO} (*Dot1l*$^{fl/fl}$ *Ddx4*-Cre^{ERT2}) testes at 35 dpt. (A, B) Immunofluorescence of DOT1L (A) and H3K79me2 (B) in control and *Dot1l*^{iKO} testes at 35 dpt. Representative tubules with a complete loss of DOT1L (A) or H3K79me2 (B) in germ cells in *Dot1l*^{iKO} testes are shown. Enlarged views of boxed cells are shown at the bottom. Abbreviations: Ley, Leydig cell; Myo, myoid cell; Ser, Sertoli cell; SC, spermatocyte; RS, round spermatid. Scale bars, 10 µm. Graphs show percentage of tubules with DOT1L-positive germ cells (A) or H3K79me2-positive germ cells (B) in control and *Dot1l*^{iKO} testes at 35 dpt. Each dot represents the percentage for one mouse. Statistics: *, $p<0.05$; **, $p<0.01$, unpaired Student's *t*-test. (C) Western blot of DOT1L, H3K79me2, ACTB, and histone H3 in testes from adult *Dot1l*$^{fl/+}$, *Dot1l*$^{fl/+}$ *Ddx4*-Cre^{ERT2}, and *Dot1l*^{iKO} males at 35 dpt. * indicates a non-specific band. (D) Relative abundance of DOT1L. Statistics: N=3, mice per genotype; **, $p<0.01$; ***, $p<0.001$; ****, $p<0.0001$, unpaired Student's *t*-test. (E) Relative abundance of H3K79me2. Statistics: N=2, mice per genotype; NS, non-significant; *, $p<0.05$, unpaired Student's *t*-test.

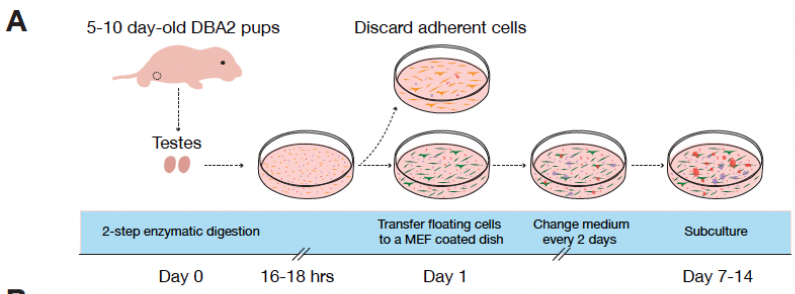

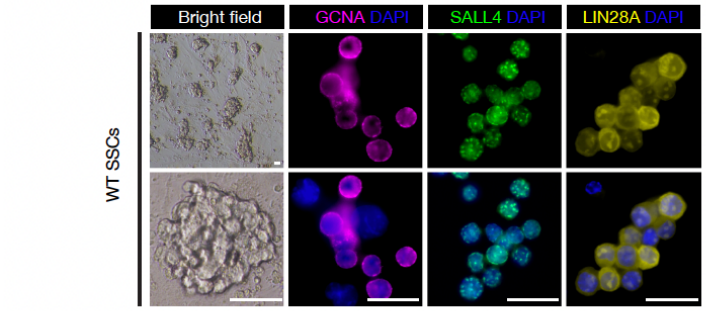

C

Up-regulated genes in EPZ5676-treated SSCs

Gene	log_2FC	log_2CPM
1700080 O16Rik	1.06	1.75
Adam22	0.87	3.49
Arnt2	0.83	4.54
AU022751	0.56	4.93
BC049730	0.93	1.31
Cntn3	0.76	3.01
Cps1	1.29	0.55
Dnah5	0.80	3.40
Elmo1	0.85	2.93
Enthd1	0.98	2.07
Frzb	0.89	2.88
Gliprl1l1	5.58	-2.22
Gm6890	0.84	2.86
Klhl1	2.60	-1.46
Msx1	3.91	-1.76
Nrk	1.31	4.06
Nrxn1	1.36	1.38
Otud6a	1.12	0.97
Peg10	0.72	6.24
Pou4f1	0.79	4.13
Ptprq	0.85	2.77
Trps1	1.15	1.11

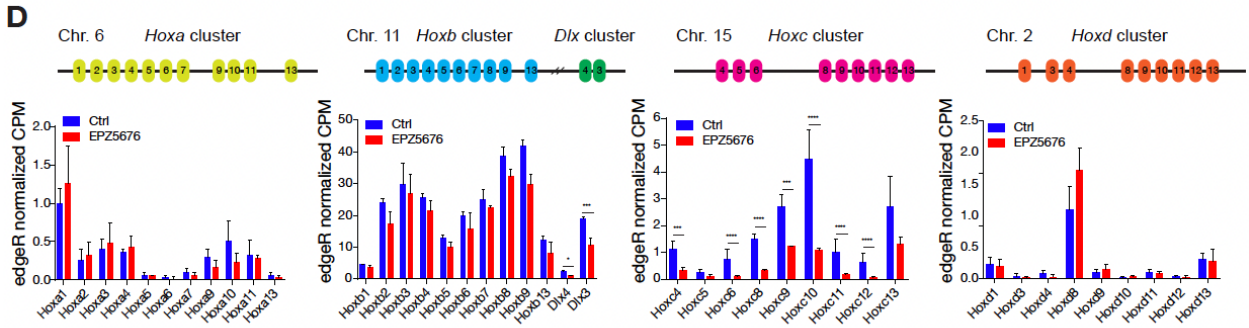

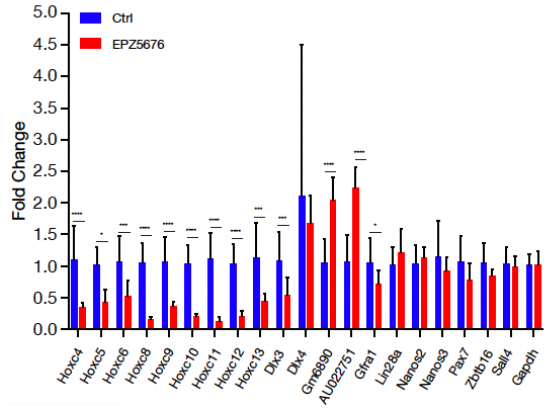

Supplemental Figure S5. Analysis of differentially expressed genes in EPZ5676-treated SSCs. (A) Scheme of establishment of SSC cultures from 5- to 10-day-old DBA2 male pups. (B) Immunofluorescence analysis of GCNA, SALL4, and LIN28A in cultured wild type mouse SSCs. (C) List of upregulated genes in EPZ5676-treated SSCs with FDR < 0.05. (D) Expression levels of all four Hox (*Hoxa*, *Hoxb*, *Hoxc*, and *Hoxd*) cluster genes and *Dlx* genes in control and EPZ5676-treated SSCs. (E) qRT-PCR analysis of *Hoxc* genes, *Dlx* genes, and known SSC genes in control and EPZ5676-treated SSCs.

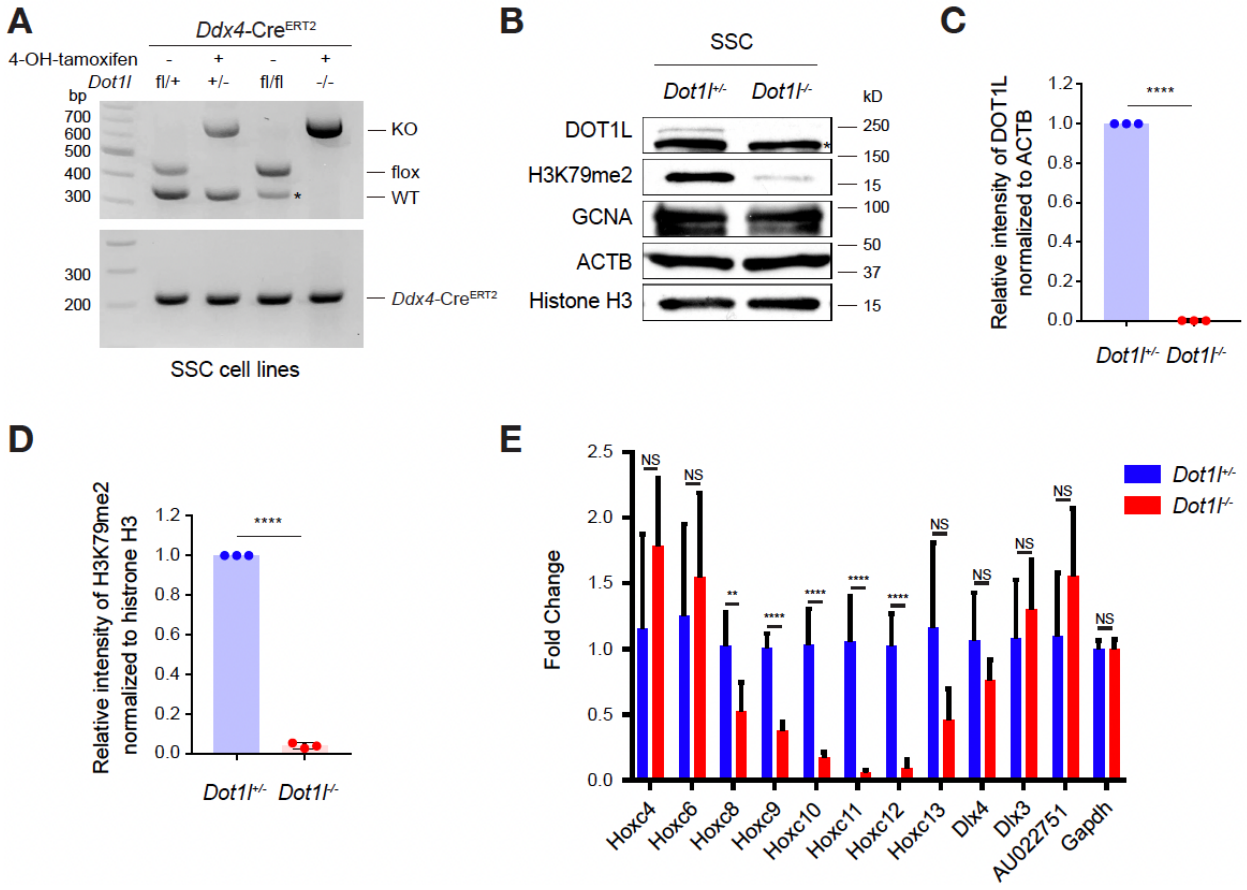

Supplemental Figure S6. Derivation and analysis of *Dot1l*$^{+/-}$ and *Dot1l*$^{-/-}$ SSC cells. (A) PCR-based genotyping of different SSC cell lines. 4-OH-tamoxifen: 4-hydroxytamoxifen. *Dot1l*$^{+/-}$ *Ddx4*-Cre^{ERT2} SSCs were derived by culturing and passaging *Dot1l*$^{fl/+}$ *Ddx4*-Cre^{ERT2} SSCs in the presence of 4-hydroxytamoxifen. *Dot1l*$^{-/-}$ *Ddx4*-Cre^{ERT2} SSCs were derived by culturing and passaging *Dot1l*$^{fl/fl}$ *Ddx4*-Cre^{ERT2} SSCs in the presence of 4-hydroxytamoxifen. Asterisk indicates a wild-type band from remnant feeder cell DNA. (B) Western blot of DOT1L, H3K79me2, GCNA, ACTB, and histone H3 in *Dot1l*$^{+/-}$ and *Dot1l*$^{-/-}$ SSCs. Asterisk indicates a non-specific band. (C, D) Relative abundance of DOT1L (C) and H3K79me2 (D). n=3, batches of SSCs. Statistics: data, average ± SD; ****, $p<0.0001$; unpaired Student's *t*-test. (E) qRT-PCR analysis of *Hoxc* genes, *Dlx* genes, and *AU022751* in *Dot1l*$^{+/-}$ and *Dot1l*$^{-/-}$ SSCs. n=3, batches of SSCs. Statistics: data, average ± SD; **, $p<0.01$, ****, $p<0.0001$, unpaired Student's *t*-test.

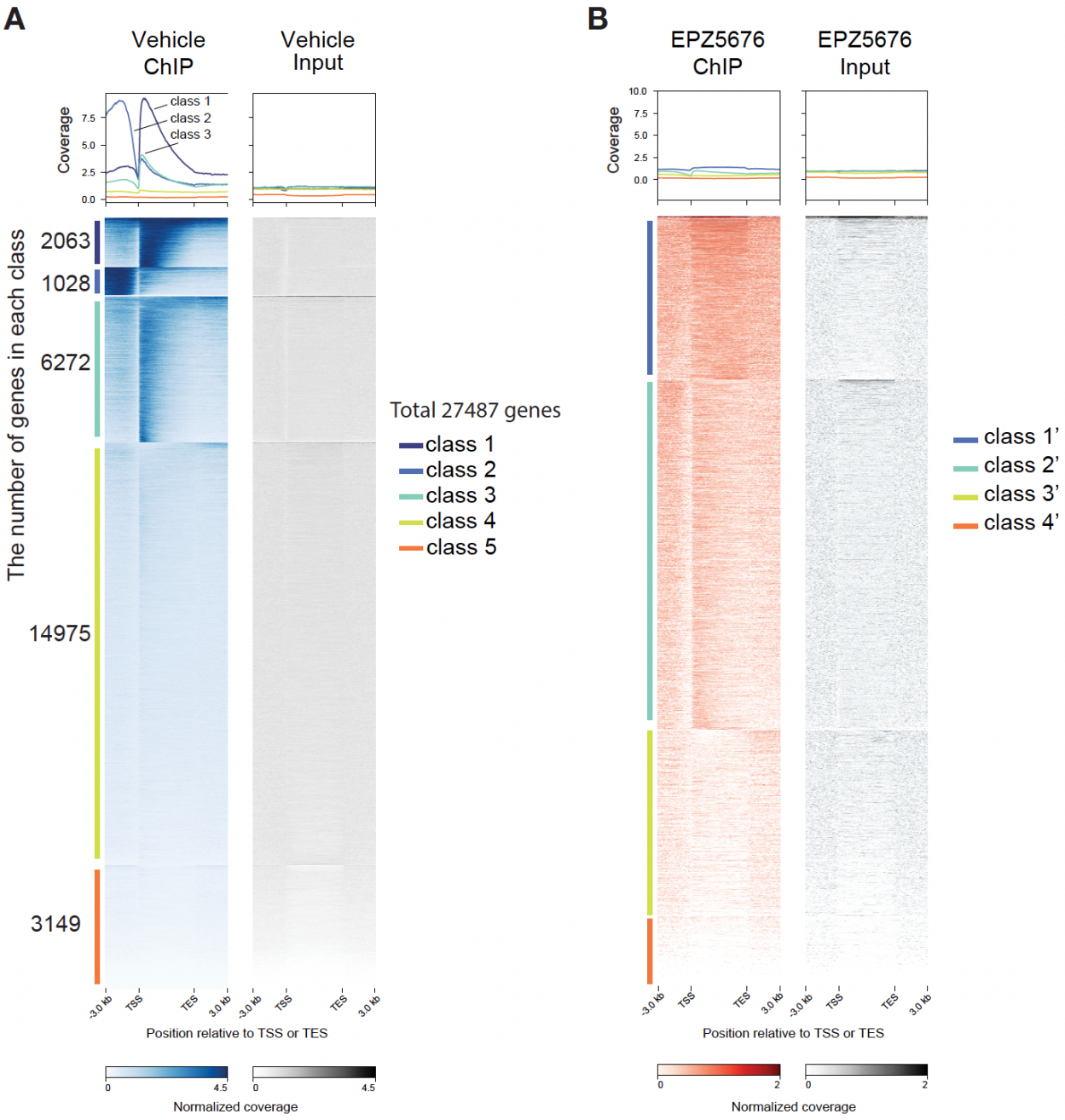

Supplemental Figure S7. Heat maps of H3K79me2 ChIP-seq data from SSCs. (A) Heatmap of distribution of the H3K79me2 ChIP-seq reads from vehicle (no inhibitor) mouse SSCs. Genes are binned to the same overall relative length. TSS: transcription start site; TES, transcription end site. Based on the heat map patterns and read density, genes are categorized into five classes. The number of genes in each class is shown. While class 1 and class 2 genes have a high level of H3K79me2 in the gene bodies or the promoters respectively, class 3 genes have a moderate level of H3K79me2 in the gene bodies. Genes in classes 1-3 are significantly enriched in H3K79me2. Input reads are shown for comparison. (B) Heatmap of distribution of the H3K79me2 ChIP-seq reads from EPZ5676-treated mouse SSCs. Input reads are shown for comparison.